MD 4145: Study of Landau damping with an Antidamper

S. Antipov, M. Albert, D. Amorim, N. Biancacci, X. Buffat, E. Carideo, E. Métral, N. Mounet, A. Oeftiger, G. Trad, D. Valuch

Summary

Landau damping is an essential mechanism for ensuring the transverse beam stability in LHC and its upgrades. It suppresses transverse head-tail modes within the bunch that cannot be otherwise damped by a narrow-band feedback or chromaticity. The goal of this study was to test an experimental procedure that would allow quantifying the strength of Landau damping using the ADT feedback as a controllable source of beam impedance. The procedure can potentially provide an accurate way of measuring the stability diagram for LHC and HL-LHC.

Contents

1 Introduction

Landau damping [1] is an essential mechanism for ensuring the transverse beam stability in LHC [2, 3], its upgrades such as HL-LHC [4], and the future high-energy hadron colliders such as FCC-hh [5]. It suppresses transverse head-tail modes within bunches that cannot be otherwise damped by a narrow-band feedback or chromaticity.

Nowadays LHC operates close to the limit of its Landau octupole system at flat-top. Precise knowledge of the amount of Landau damping is key to making accurate predictions on beam stability as the ring is gradually upgraded for the future high intensity operation.

The studied novel approach for measuring the strength of Landau damping involves using the transverse feedback with the reverted polarity (anti-damper) to act as a controllable source of beam impedance. By knowing the strength of the feedback excitation, and observing at which gain the beam becomes unstable, one obtains a direct measurement of the strength of Landau damping in the ring.

The MD was divided into two parts. The first part focused on calibrating resistive and reactive components of damper gain that were later used in experiment. Ensuring an accurate control over both phase and gain of the feedback was of paramount importance for exploring the stability diagram and benchmarking with simulation predictions. The second part of the MD focused on proof of principle tests to measure the strength of Landau damping created by the rings octupole system.

2 Feedback as Controlled Impedance

If a variation of the damper's dynamic response over the bunch length can be neglected (which is true for LHC transverse feedback whose bandwidth goes up to 40 MHz or 1 RF bucket), i.e. it is 'flat', it can be described as a constant wake force acting on the beam $W(z) = W_0 = const$. This wake corresponds to a δ-function-like coupling impedance (for reference see, for example, [6]):

$$Z_{ADT}(\omega) \sim i g_{ADT} e^{i\phi_{ADT}} \times \delta(\omega), \tag{2.1}$$

where g_{ADT} stands for feedback gain in inverse turns and ϕ_{ADT} - its phase: 0 for a resistive feedback (acting on beam position) and 90 deg for a reactive one (acting on transverse beam momentum). A resistive feedback thus drives a coherent beam mode upwards in the diagram, driving it unstable, with an instability growth rate of $-g_{ADT}$.

A realistic impedance of various accelerator components ranges from inductive impedance of high-Q RF modes, to 50/50 real and imaginary impedance of resistive collimator jaws, to purely imaginary impedance of bellows and tapers. These tune shifts can be modelled by different phases of the damper: 0 for purely imaginary tune shift and 90 deg for purely real, as shown in Fig. 1.

2.1 Choice of parameters

In order to make a clean measurement one has to make sure there is only one dominant head-tail mode and no interference from the others is possible. Such interference may lead one or another mode crossing the Stability Diagram, depending on the exact value of damper phase, chromaticity, or beam intensity, greatly complicating the analysis. For example, for LHC at Top energy (6.5 TeV, $Q' = 15$) there is only one dominant azimuthal mode at the nominal intensity (-1), while there may be two modes with similar growth rates (0, and -1) at half the nominal intensity (see Appendix A).

At LHC injection energy with probe beams the dipolar, 0 mode, typically dominates the landscape with other modes being sufficiently below it (Fig. 2). Working with probe beams allows minimizing mode shift from beam coupling impedance as well space charge effects (discussed below in more detail). At the same time, thanks to the low beam energy, one can easily create a large octupole tune shift to
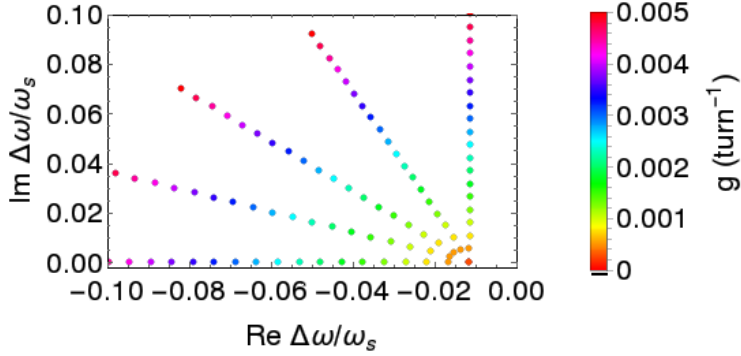
Figure 1: Simulated real (horizontal) axis and imaginary (vertical) axis frequency shifts of mode 0, normalized by the synchrotron frequency, as a function of ADT feedback gain for 5 equidistant values of phase between 0 and 90 deg.
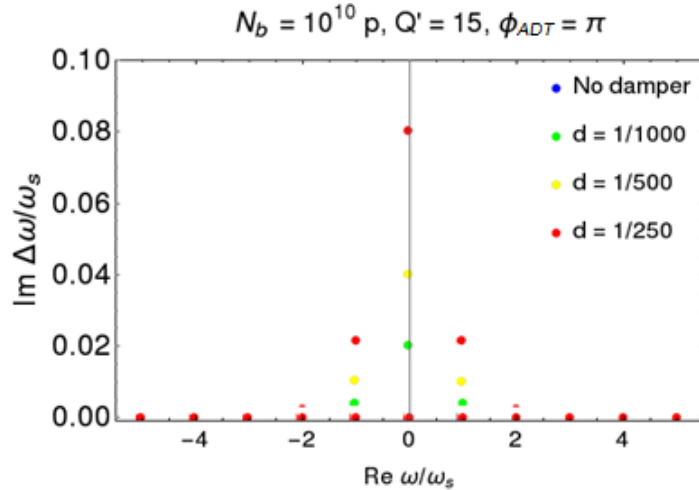

Figure 2: Azimuthal mode 0 dominates the growth rate as the negative damper gain is increased with probe beams at injection energy. Real and imaginary tune shifts are normalized by the synchrotron frequency.

stabilize the beam without the feedback, which is handy when setting up the measurement. Table 1 summarizes the key parameters chosen for the MD.

2.2 Impact of space charge

Although space charge on its own does not create Landau damping for mode 0, as pointed out by Möhl [7], it modifies the stability diagram produced by lattice nonlinearities. Its impact can be estimated analytically in a simple model [8], assuming a quasi-parabolic transverse distribution, coasting beam, and a linear space charge detuning. These assumptions are valid when the strength of space charge detuning is small relatively to other sources. In general, an interplay of octupole detuning and nonlinear space charge may be important as observed in particle tracking simulations [9]. Note that the model can be readily extended to bunched beams as prescribed by Ng [10], although the impact of the bunching is minor. Depending on the strength of the space charge, it leads to a shift of the stability diagram maximum towards negative tune shifts, widening of the diagram, and a slight reduction of its height.
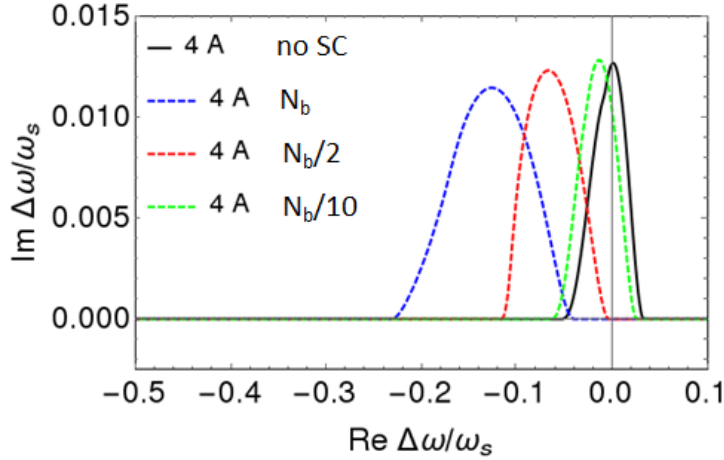
Figure 3: Example stability diagrams at injection energy without (black line) and with (color lines) space charge interaction for a Nominal intensity of 1.15×10^{11} ppb and a positive octupole current of 4 A. The shift Δ_0 for the Nominal intensity can be as large as 10^{-3}, whereas for the 10 times smaller Probe intensity it does not exceed 10^{-4}; 2.5μm emittance is assumed.

For the studied parameters, the space charge is relatively weak and provides only a measurable shift of the stability diagram of around $\Delta_0 = 10^{-4}$ while leaving its width and height roughly the same (Fig. 3).

2.3 Impact of lattice nonlinearities

A major part of lattice nonlinearities in LHC is created on purpose by its octupole system, which creates an rms detuning of the order of 10^{-4} at injection in normal operation. The octupoles are typically much stronger than the natural lattice nonlinearities, which are roughly equivalent to about -2.5 A of octupole detuning and provide $\sim 10^{-5}$ rms tune spread [11]. The natural nonlinearities can therefore be safely omitted from the analysis, at least in first order, except for the case of 0 current.

Parameter	Value
Beam energy	450 GeV
Beam intensity	0.5×10^{10} ppb
Number of bunches	1
Norm. emittance, rms	1.0-1.1 μm
Bunch length, $4\sigma_{rms}$	1 ns
Coupling	0.001
RF voltage	6 MV
Tunes, x, y, z	0.275, 0.295, 0.005
Synch. freq., ω_s	0.03 rad^{-1}
SC tune shift	10^{-4}

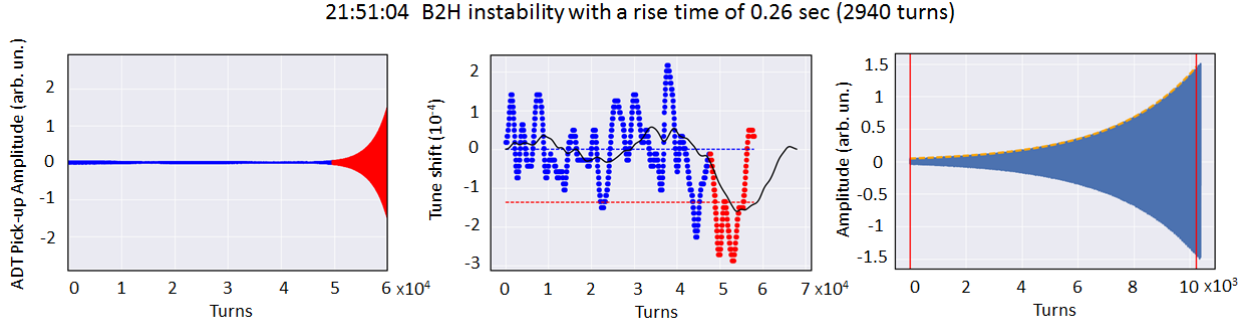Table 1: Key parameters used for the study

Figure 4: An example of ADT data for a 45 degree phase. Left - oscillation envelope over 64000 acquisition turns, the unstable area, defined by a crossing of the threshold, is shown in red. Center - tune variation over time, obtained with a moving FFT window of 2000 turns; solid black line shows the moving average, dashed blue - average stable tune, dashed red - average unstable tune. Right - exponential amplitude blow-up observed in the unstable region; the exponential fit with a time constant of 2940 turns is shown in orange.

3   Measurement Procedure

A proof-of-principle test was performed at the nominal LHC injection settings with an injection probe beam: a single bunch of 0.5×10^{10} p in 1 μm normalized rms emittance (Table 1). Usage of the nominal settings was imperative in order to ensure a rapid machine set-up and reinjection, needed for repetitive measurements, as well as precise control of the optics. The MD took two Fills spread over 6 hours of LHC operation: Fill 7387 where the ADT was set up and the following Fill 7388 where most of the measurements were taken, and was performed in Beam 2 in parallel to the Q22 transfer line MD that worked with Beam 1. Apart from a brief power glitch between the two fills, we were able to use all the available time to full extent, thanks to excellent work and cooperation of LHC and injectors OP crews.

First, the feedback was calibrated and qualified to act as an effective impedance, and then it was used to measure Landau damping in several configurations of octupole current and polarity.

3.1   Feedback calibration

The feedback system was calibrated with no octupole current at three anti-damper phases: 0, 45 and 65.7 deg. The calibration was required to make sure of the independent control over the damper gain and phase. Figure 4 shows a sample dataset for a phase of 45 deg and a gain of 0.009 units. More examples of data can be found in Appendix B.

The resulting dependence of the instability growth rate on the feedback gain was found to be linear, as expected (Fig. 5), with the slope reducing gradually with the phase, also as expected. The magnitude of the slope yields the calibration factor for the damper gain (i.e. an ADT with a setting of x units drives an instability with an exponential rise time of y turns) for the following measurements.

The sign of the tune shift was verified by BBQ, although no on-the-fly analysis of the tune shift was done, as it was complicated by the presence of tune jitter. A significant tune jitter of the order of 1×10^{-4} is present in the data (Fig. 6, center). An accurate reconstruction of the tune turned out to be possible only for a phase of 45 deg, where the tune shift is large enough to overcome the noise and, an the same time, the instability growth rate is slow enough to mitigate the tune drift. As expected, the tune varies linearly with the feedback gain, and its slope matches what one would expect from the growth rate measurement: 1.3×10^{-2} vs $\frac{1}{2\pi}6.39 \times 10^{-2} = 1.0 \times 10^{-2}$ (Fig. 6). A small discrepancy can be explained by the uncertainty of tune shift determination. An uncertainty in damper phase can also contributes
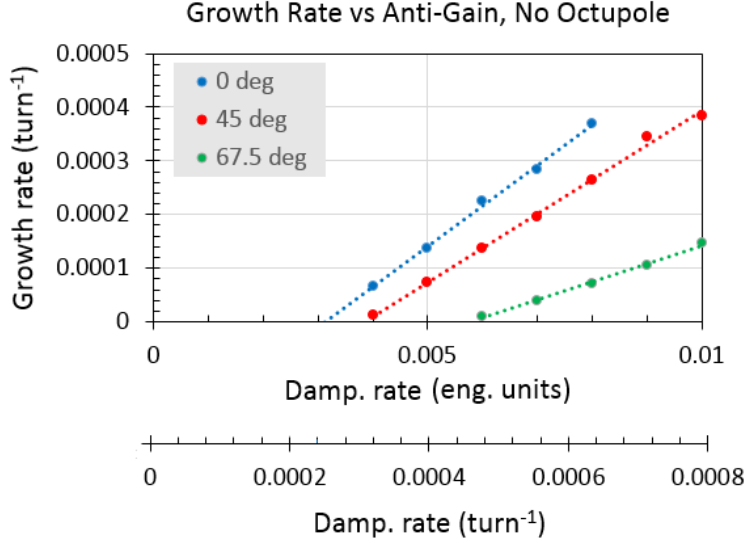
Figure 5: Instability growth rate scales linearly with the damper gain, allowing to calibrate the ADT strength. The non-zero gain required to start an instability is caused by natural nonlinearities of the machine.

to the difference but it is rather small, less than 1 deg, according to ADT data post-processing (see Appendix C).

Damper phase	Growth rate	Tune shift
0 deg	7.53×10^{-2} 1/turn/eng. un.	N/A
45 deg	6.39×10^{-2} 1/turn/eng. un.	-1.3×10^{-2} 1/eng.un.
67.5 deg	3.39×10^{-2} 1/turn/eng. un.	N/A

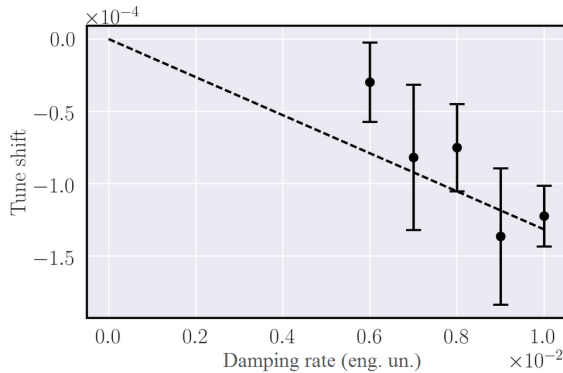Table 2: Summary of feedback gain calibration

Figure 6: Mode 0 (center-of-mass) tune shift increases linearly with damping rate at the phase of 45 deg. Dashed line representing a fit $\delta Q = a \times g_{ADT}$ allows an independent calibration of the ADT strength by the produced tune shift.
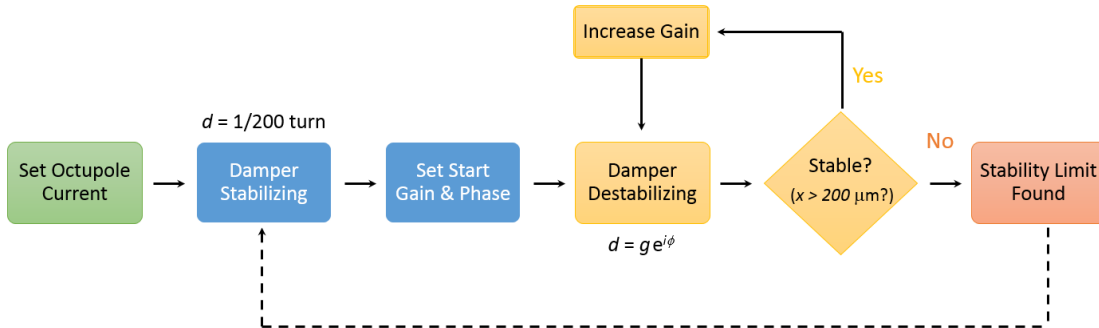
6

Figure 7: Procedure for measuring stability diagrams: damper gain is increased at a fixed phase until a threshold amplitude is exceeded then the damper is reverted back to stabilizing.

3.2 Stability Diagram scans

After calibrating the anti-damper we performed a series of measurements at different octupole settings. At each setting the damper gain was gradually increased in small steps until reaching the limit of stability, then its phase was increased and the procedure repeated for at least 5 phases between 0 and 90 deg.

We used an automated script, developed by D. Valuch, to perform the scan. At each step the feedback gain was kept constant for about 30 sec, which should have excluded potential impact of latency effects as they were not observed in recent single bunch octupole threshold measurements with sufficiently short, about 1 min steps [12]. An instability was declared if a beam centroid excursion from the reference orbit exceeded 200 μm. In that case, the damper was automatically switched back to a resistive stabilizing one, and the last 64k turns of ADT data were saved for future processing. This procedure, schematically depicted in Fig. 7, allowed locating the boundary of stability typically within 5 min.

At injection the beam emittance was usually between 1 and 1.1 μm (measured by BSRT). Normally, it was not affected by the measurement, although in certain cases a blow-up was observed. Then, if beam emittance increased by over 10%, i.e. exceeded 1.2 μm, we would reinject the beam. Not reinjecting the beam for each data point allowed drastic time savings during the MD. The downside of this approach is that the distribution tails, which have a large tune shift and thus play a large role in Landau damping, might have been affected by the previous instabilities. A change in tail population could then affect subsequent measurements of instability thresholds. While several data points were measured twice: with a 'old' and with a 'fresh' beam and the results were in good, 10% or better agreement, no systematic study of the effect was attempted this time.

Before performing the measurements coupling was measured. Its value $C^- = 0.001$, i.e. the global coupling defined as the closest tune approach, was considered sufficiently low and no corrective action was taken. Longitudinal bunch length was also measured and found to be 1 ns ($4\sigma_{rms}$). Chromaticity measurement was done later in the MD; it turned out to be +14 units with a reasonable uncertainty estimate of ± 1 unit. We performed scans at this nominal chromaticity for octupole knob values corresponding to +11, +17, and -11 A; then at the end of the MD the Q' was corrected down to +3 units and the measurement at +11 A was repeated.

4 Results and Discussion

In this section we discuss the results of measurements of stability diagrams at different octupole and chromaticity settings at injection energy and provide an estimate of its fill-to-fill variation arising from slight differences in beam parameters.
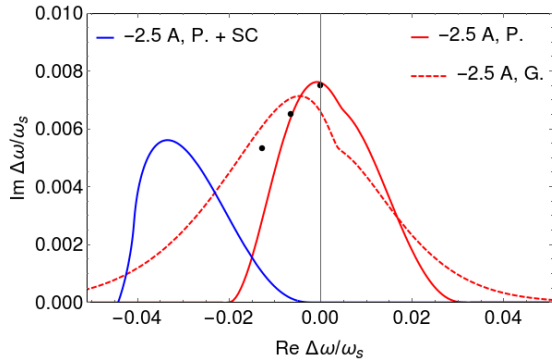
Figure 8: Measured Stability Diagram from natural machine nonlinearities for Beam 2 at 450 GeV (black dots). Red lines show SD predictions without space charge: solid one for a quasi-Parabolic distribution cut at $3.2\sigma_{rms}$ and dashed - Gaussian; the solid blue line represents SD prediction for a Parabolic distribution and linear space charge detuning. Real and imaginary tune shifts are normalized by the synchrotron frequency.

4.1 Natural nonlinearities

The calibration plot in Fig. 5 gives an insight into the strength of Landau damping by natural non-linearities of the lattice, which is given by the intersection of the lines with the horizontal axis. These are the points where the beam as a dynamical system is exactly at the limit of stability. An excitation anti-damping rate of about $2.5 \times 10^{-4} = 1/4000$ turn^{-1} is needed to destabilize the beam. Figure 8 shows the dependence of the instability growth rate on the complex damper gain $g_{ADT}e^{i\phi_{ADT}}$ and the corresponding stability diagram found by extrapolating to Im $\Delta Q = 0$. The height of the resulting stability diagram matches what one would expect from a -2.5 A octupole equivalent, with the shape of the stability curve being between a pure Gaussian and that of a quasi-Parabolic transverse distribution.

The space charge interaction, in a linear model, should have significantly shifted the stability diagram towards negative frequencies, making all the measured points unstable. That effect, however, has not been observed in the experiment (Fig. 8). An important missing ingredient might be the longitudinal variation of the transverse space charge forces that increases the tune spread towards positive values and thus increases the stability region on the right-hand side, as noted in [8].

To investigate the issue further we performed macroparticle simulations in PyHEADTAIL. The numerical model included a -2.5 A equivalent octupole nonlinear amplitude detuning, nonlinear longitudinal motion, but no space charge interaction. Just as in the experiment, in simulation the instability growth rate scaled linearly with the negative damper gain (Fig. 9, left). Surprisingly though the tracking simulation predicted a lower stability threshold than the one observed in the measurement and the one expected from a naive SD point of view (Fig. 9, right). The SD height in the tracking simulation is around a factor two smaller than the measured one. This discrepancy can be caused by non-octupolar terms of lattice nonlinearities that are not accounted in the numerical model. A further investigation, including nonlinearities and longitudinal momentum spread (contributing to Landau damping via Q'') is required.

Injection-to-injection spread of the strength of Landau damping, measured over 5 consecutive injections at 11 A and 0 deg phase (resistive anti-damper) turned out to be rather small - around 7%, indicating a quite good reproducibility of beam distribution. The 7% value gives lower limit of the systematic uncertainty in all the subsequent measurements. Depending on the direction of the shift the modes would probe different parts of the octupole stability diagram: for the imaginary shift it would be the center that is nearly independent of the beam distribution or the octupole polarity, whereas for the real shift it would be the tail of the diagram that drastically depends on the beam parameters (i.e.
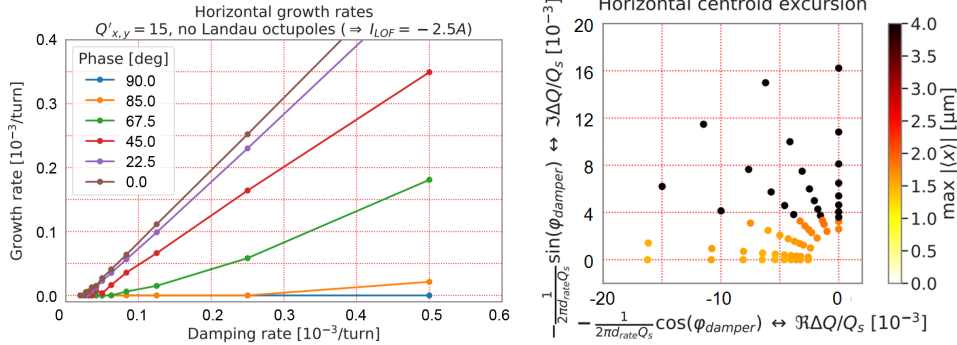
Figure 9: Simulated instability growth rate as a function of anti-damper gain for natural lattice nonlinearities at injection energy. Left - growth rate of mode 0 for different damper phases; right - complex plane footprint showing the region of beam stability. Gaussian transverse distribution with $\epsilon_n = 1.0\ \mu m$.
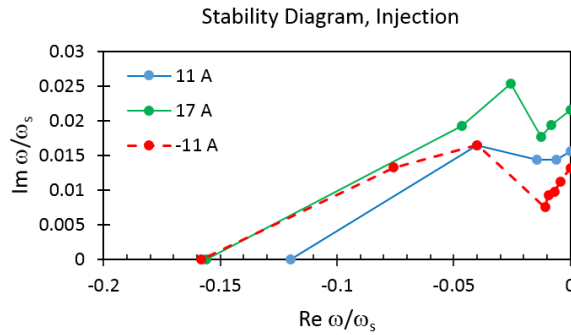

Figure 10: Measured stability diagrams for Beam 2 at 450 GeV; horizontal plane, $Q' = 14$. The height of the diagrams scales linearly with the octupole current. Negative octupole polarity offers around 30% larger coverage of negative tune shifts, which are relevant for coherent beam stability. Real and imaginary tune shifts are normalized by the synchrotron frequency.

emittance, intensity, bunch profile, etc.), which all vary slightly fill-to-fill. The uncertainty of the SD tails can therefore be significantly larger than that of for the central peak.

The shape of the measured stability diagrams at 11, 17, and -11 A qualitatively matches the expectations from a simple linear Stability Diagram (SD) theory. Quantitatively, both the height and the width scale with the octupole current, with the SD for 17 A being around 50% higher than that for 11 A, as expected (Fig. 10). It is worth noting that the negative octupole polarity offers around 30% greater coverage of the negative tune shifts, also in good qualitative agreement with expectations. This illustrates why the negative polarity is preferred to suppress impedance-driven instabilities in LHC that feature negative mode frequency shifts. The exact magnitude of the gain should depend on the details of beam distribution.

When compared with the theoretical predictions in the linear space charge approximation mentioned above, experimental data shows around a factor two lower stability thresholds then those predicted by Stability Diagrams (Fig. 11). Studies show that a change in amplitude detuning with octupole current is in good agreement with expectations [13]. A part of the discrepancy could come from a larger than expected lattice nonlinearities that are relatively strong at injection energy. Normally, uncorrected lattice nonlinearities produce several amps of extra equivalent octupole detuning in the arcs at injection compared to magnetic model.

There are several sources affecting Landau damping at injection energy. The first one is hysteresis effect of the octupole correctors affecting their magnetic field. It is responsible for a systematically larger

9

than predicted Q'' measured in the machine [14]. In 2018 the octupole correctors were turned off and therefore no impact from this source is expected. Another significant effect is the linear coupling that can change amplitude detuning from Landau octupoles, reducing the footprint locally, but leading as well to a large second order amplitude detuning [15, 16]. It is important to note that the value of C^- may change by as much as 5×10^{-3} over several hours at injection if uncorrected, which is with alignment errors of sextupole spool pieces [17]. In this test the coupling has been corrected only once and not throughout the measurement and could have drifted away from the initially measured value of 10^{-3}. Another issue identified in [15] is the large working point-dependent nonlinear amplitude detuning in the plane where one approaches the coupling resonance. This should not have been an issue for the present measurement as the real tune shifts during stability diagram scans did not exceed 0.001. Finally, recent findings indicate a potential feed-down from decapole MCD correctors due to their supposed systematic misalignment of about 0.25 mm [18].
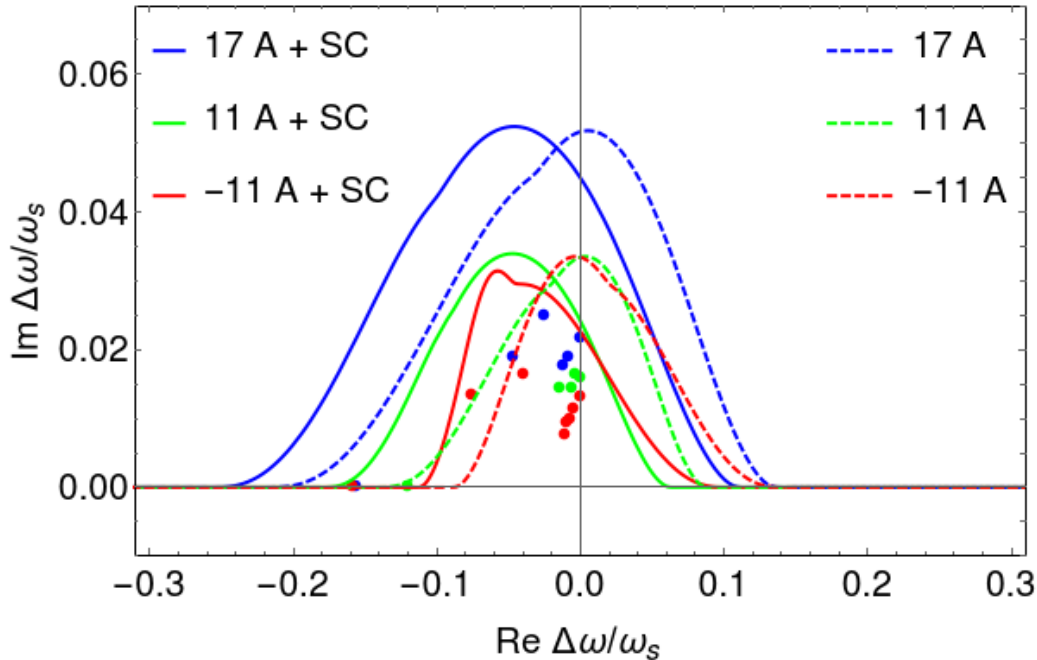

Figure 11: Experimental data (dots) suggest a lower amount of Landau damping than the corresponding Stability Diagrams (lines). Dashed lines represent SDs for a parabolic transverse distribution cut at $3.2\sigma_{rms}$ without space charge, and solid - with SC. Beam 2, injection energy, horizontal plane. Real and imaginary tune shifts are normalized by the synchrotron frequency.

4.2 Landau damping at Q' near 0

Surprisingly, at first sight, the beam became unstable at a lower damper gain at a Q' around 0 than at $Q' \sim 15$. While this finding goes in the direction of higher stability thresholds observed near $Q' \sim 0$ in the past, it is not expected from a simple stability diagram theory, and had to be understood. Figure 12 shows a comparison of simulated unstable modes between the measured chromaticities 3 and 14. The simulation includes the effect of machine impedance, but not the space charge. Due to lower chromaticity the azimuthal mode 0 has a higher growth rate at $Q' = 3$ with modes ± 1 nearly invisible. This higher growth rate at low chromaticities has not been accounted for in the damper calibration that was performed at $Q' = 14$ and seems to be the cause of the discrepancy.

Since there was no calibration performed at $Q' = 3$ we used simulation data to recalculate the mode

0 growth rate for the measured data point. When corrected for the actual mode 0 growth rate the measurements at the two chromaticities are in a good quantitative agreements with each other (Fig. 13).
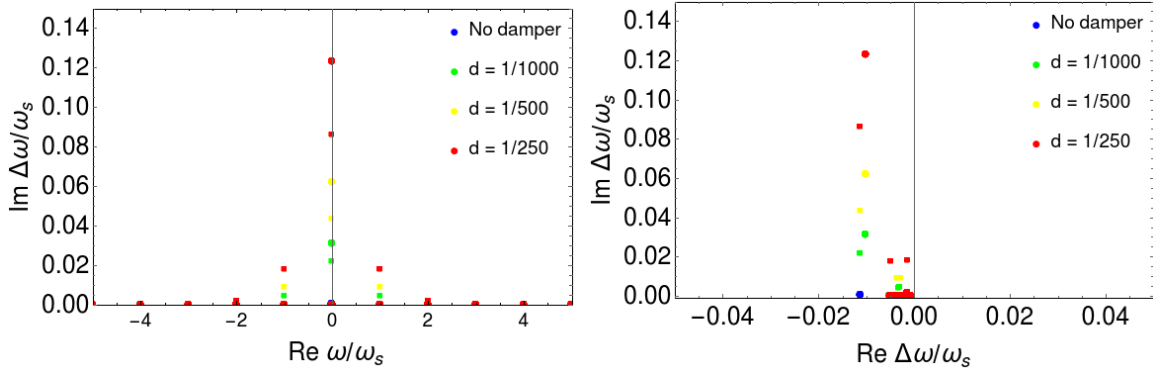

Figure 12: Azimuthal modes for $Q' = 14$ (circles) vs modes for $Q' = 3$ (squared) and different damper gains: the mode 0 is around 45% lower at the larger chromaticity. Left – growth rates of unstable azimuthal modes as a function of their frequency; the modes are grouped by their azimuthal numbers around frequencies $l\omega_s$. Right – their complex tune shifts (with respect to $\omega = l\omega_s$).
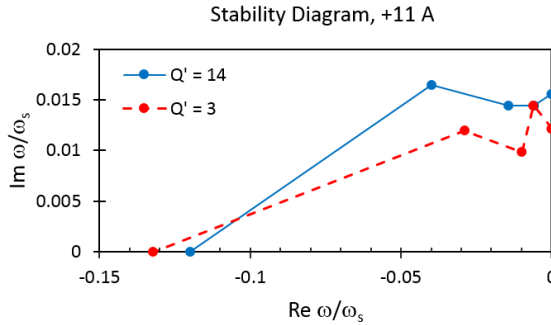

Figure 13: Stability diagram for $Q' = 14$ seems to match that of $Q' = 3$ after correction for the higher mode 0 growth rate at lower chromaticities. Beam 2, injection energy, horizontal plane. Real and imaginary tune shifts are normalized by the synchrotron frequency.

5   Conclusion and Outlook

In this MD we have demonstrated that the active feedback system can be used as a source of controlled impedance to probe the strength of Landau damping. The proof-of-principle experiment has been carried out in LHC at injection energy with single pilot bunches.

First, the ADT feedback has been calibrated to create an arbitrary complex tune shift. The ADT demonstrated a precise control of excitation rate in a wide range of gains from $\sim 10^4$ to $\sim 10^3$ turn as well the phase, which could be set with a precision of better than 1 deg. Both tune shift and instability growth rate have been demonstrated to increase linearly with the feedback gain, as expected. In general, calibrating the feedback at lower chromaticities and lower beam intensities seems preferable, since it allows minimizing the effects of space charge and impedance detuning. A good control and an accurate knowledge of natural machine nonlinearities seems important for being able to benchmark the results against Stability Diagram predictions.

Then, the feedback has been utilized to directly measure the strength of Landau damping by gradually increasing its gain until a transverse activity is observed. The implemented procedure seems to be fast, requiring only several minutes, and non-destructive for the beam. The possibility of exploring the stability diagram by changing the damper phase has also been demonstrated. The results are in good qualitative agreement (within a factor two) with the theoretical SD predictions. A detailed quantitative analysis (in particular, tracking simulations with space charge) is required to include effects of lattice nonlinearities and coherent effects in the picture. Understanding and precise control of lattice nonlinearities and coupling would also be beneficial in case of repeating the measurement in the future as they might significantly affect the tune footprint. With a beam-based nonlinear correction one should be able to keep the lattice nonlinearities at injection at a sub 1 A level, as seen in 2016-17 [13].

The technique has a potential to become a fast non-destructive tool for measuring the strength of Landau damping throughout the accelerator cycle. In particular, it would be well suited for studies at Flat-Top, where the constraints arising from Landau damping are the tightest and the effect of space charge is negligible. In order to explore this potential, further studies including the top energy of 7 TeV are required after the Long Shutdown.

Acknowledgments

References

[1] L. D. Landau, "On the vibrations of the electronic plasma," J. Phys. (USSR) **10**, 25 (1946) [Zh. Eksp. Teor. Fiz. **16**, 574 (1946)].

[2] O. S. Brüning, P. Collier, P. Lebrun, S. Myers, R. Ostojic, J. Poole and P. Proudlock, "LHC Design Report Vol.1: The LHC Main Ring," doi:10.5170/CERN-2004-003-V-1

[3] J. Gareyte, J. P. Koutchouk and F. Ruggiero, "Landau damping, dynamic aperture and octupoles in LHC," CERN-LHC-PROJECT-REPORT-091

[4] G. Apollinari, I. Béjar Alonso, O. Brüning, M. Lamont and L. Rossi, "High-Luminosity Large Hadron Collider (HL-LHC) : Preliminary Design Report," doi:10.5170/CERN-2015-005

[5] A. Abada *et al.* [FCC Collaboration], "Future Circular Collider : Vol. 3 The Hadron Collider (FCC-hh)," CERN-ACC-2018-0058.

[6] A. Burov, "Nested Head-Tail Vlasov Solver," Phys. Rev. ST Accel. Beams **17**, 021007 (2014) doi:10.1103/PhysRevSTAB.17.021007 [arXiv:1309.0044 [physics.acc-ph]].

[7] D. Möhl, "On Landau damping of dipole modes by nonlinear space charge and octupoles," Part. Accel. **50**, 177 (1995).

[8] E. Métral and F. Ruggiero, "Stability diagrams for Landau damping with two-dimensional betatron tune spread from both octupoles and non-linear space charge," CERN-AB-2004-025-ABP.

[9] V. Kornilov, O. Boine-Frankenheim and I. Hofmann, "Stability of transverse dipole modes in coasting ion beams with nonlinear space charge, octupoles, and chromaticity," Phys. Rev. ST Accel. Beams **11**, 014201 (2008). doi:10.1103/PhysRevSTAB.11.014201

[10] K. Y. Ng, "Landau damping of space-charge dominated Fermilab Booster beam," FERMILAB-CONF-08-410-AD.

[11] E. H. Maclean, Private communication, 2019

[12] X. Buffat, *et al.*, "Summary of instability observations at LHC and implications for HL-LHC," CERN, 9 Jul 2019, `https://indico.cern.ch/event/831847/`

[13] E. H. Maclean, *et al.*, "Tune-footprint through the LHC cycle," CERN, 17 Oct 2017, `https://indico.cern.ch/event/672805/`

[14] M. McAteer, *et al.*, "Magnet polarity checks in the LHC," CERN-ACC-NOTE-2014-0012, `http://cds.cern.ch/record/1667590/files/CERN-ACC-NOTE-2014-0012.pdf`

[15] E. H. Maclean, R. Toms, F. Schmidt and T. H. B. Persson, "Measurement of nonlinear observables in the Large Hadron Collider using kicked beams," Phys. Rev. ST Accel. Beams **17**, no. 8, 081002 (2014).

[16] E. H. Maclean, F. Carlier, M. Giovannozzi, T. Persson and R. Tomàs, "Effect of Linear Coupling on Nonlinear Observables at the LHC," doi:10.18429/JACoW-IPAC2017-WEPIK092

[17] T. Persson, Private communication, 2019

[18] E. H. Maclean, "Observations relating to MCDO alignment," CERN, 5 Feb 2019 `https://indico.cern.ch/event/812944/`

A   Interference from Multiple Unstable Azimuthal Modes

At a nominal beam intensity and relatively high chromaticity there may be several azimuthal modes with similar growth rates. Which of them becomes unstable first in the measurement is then determined by the shape of Stability Diagram and mode frequency shift from impedance (Fig. 14). While, in principle, these effects can be simulated (i.e. using a Vlasov solver) they add unnecessary parameters, that might be not very well known or poorly controlled, in the picture. Therefore such interference of different modes should be avoided when designing the experiment.
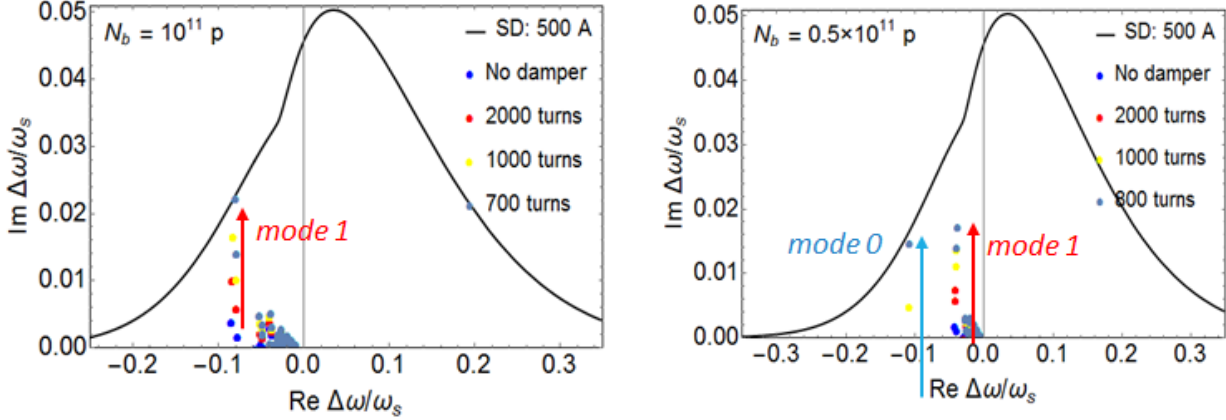

Figure 14: At Top energy and Nominal machine settings there could be several interfering modes with similar growth rates, depending on beam intensity. Left - nominal intensity of 10^{11} ppb, right - half the beam intensity. $E = 6.5$ TeV, $Q' = 15$, $I_{oct} = +500$ A, $\epsilon_n = 2.5$ μm, nominal collimator settings.

B   ADT Data

An example of ADT data for the 45 deg phase, obtained during feedback calibration when increasing the gain from 0.006 to 0.010 units (Fig. 15). Turn-by-turn data was gathered for 64000 turns for each event.

C   ADT Phase Setting Error

In normal operation the ADT phase setting is optimized for a particular tune value. When operating away from the optimal tune, the phase of the pickup signal receives an error with respect to an ideal value. The error is 0 for 0 and $\pi/2$ phase shifts and is the greatest for $\pi/4$. For the MD parameters with the tune close to 0.27 the should have never exceeded 4 deg (Fig. 16). It must be noted, that since the error has a signal processing nature, it is deterministic, that is it can be, in principle, computed in simulation and taken into account for every measurement data point.

   The impact of the pickup phase error on the ADT phase seen by the beam is actually smaller, since the damper sums signals from two pickups, each with a different relative phase to the kicker. Processing the raw ADT data we obtain that for all working points used in the MD, the absolute errors are always a very similar value, but opposite sign, almost cancelling each other. The remaining phase error is a small fraction of a degree, as can be seen in Table 3

Tune setting	$\Delta Q7$ (deg)	$\Delta Q9$ (deg)	ADT Phase error (deg)
0.260	3.4	-3.2	0.2
0.265	3.2	-3.1	0.1
0.270	3.0	-2.8	0.2
0.275	2.8	-2.6	0.2
0.280	2.5	-2.3	0.2
0.285	2.1	-1.9	0.2
0.290	1.7	-1.6	0.1
0.295	1.3	1.2	0.1

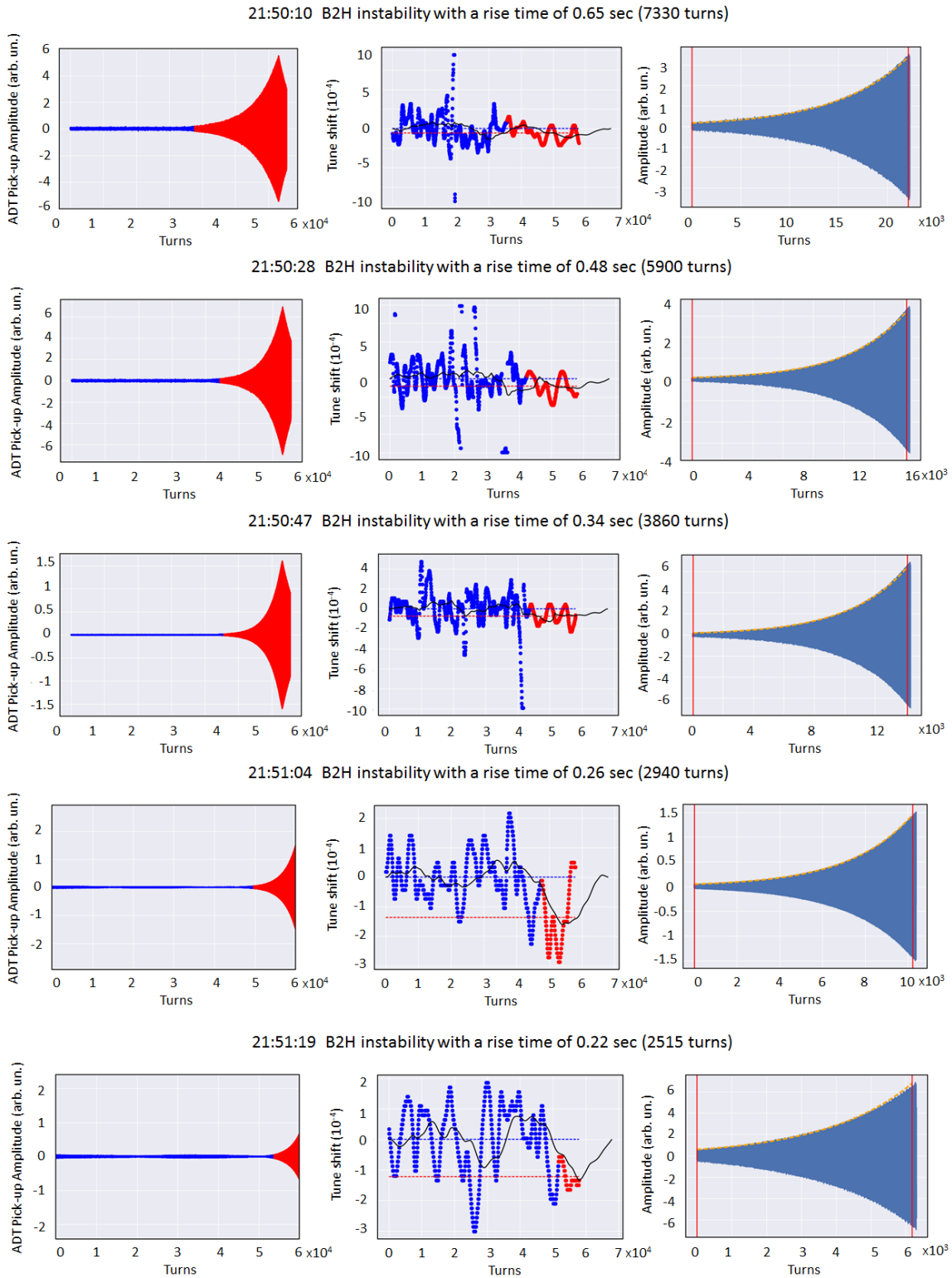Table 3: ADT pickup phase shift and kick errors. Nominal ADT setting is $Q7 = -26.0$ deg, $Q9 = 69.0$ deg.

Figure 15: ADT data for a 45 degree phase. Left – oscillation envelope over 64000 acquisition turns, the unstable area, defined by a crossing of the threshold, is shown in red. Center – tune variation over time, obtained with a moving FFT window of 2000 turns; solid black line shows the moving average, dashed blue – average stable tune, dashed red - average unstable tune. Right – exponential amplitude blow-up observed in the unstable region; exponential fits are shown in orange.
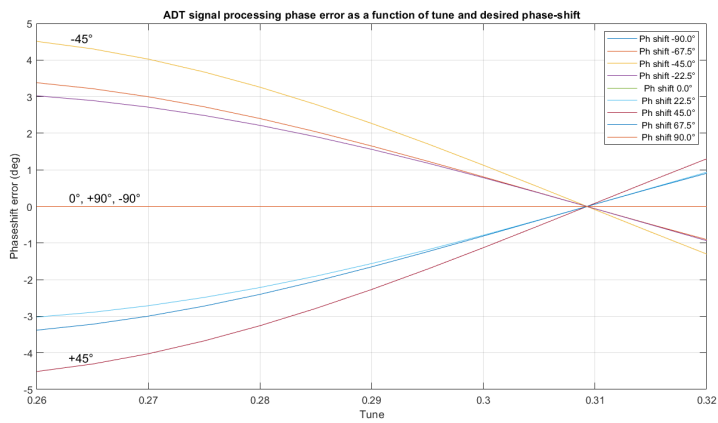
Figure 16: ADT signal processing phase error as a function of tune (horizontal axis) and the requested phase shift (colored traces) in a range from -90 to +90 degrees.